Supplementary Information

Identification of LASSBio-1945 as an Inhibitor of SARS-CoV-2 Main Protease (M^{PRO}) Through *In Silico* Screening Supported by Molecular Docking and Fragment-Based Pharmacophore Model

Lucas S. Franco,[b,c] Rodolfo C. Maia,[a,c] and Eliezer J. Barreiro*[a,b,c]

[a] Instituto Nacional de Ciência e Tecnologia de Fármacos e Medicamentos (INCT-INOFAR; http://www.inct-inofar.ccs.ufrj.br/), Universidade Federal do Rio de Janeiro, CCS, Cidade Universitária, Rio de Janeiro, RJ, Brazil.

[b] Programa de Pós-Graduação em Farmacologia e Química Medicinal, Instituto de Ciências Biomédicas, Universidade Federal do Rio de Janeiro, Avenida Carlos Chagas Filho, 373, Ilha do Fundão, 21941-912, Rio de Janeiro, RJ, Brazil.

[c] Laboratório de Avaliação e Síntese de Substâncias Bioativas (LASSBio®, http://www.lassbio.icb.ufrj.br), Instituto de Ciências Biomédicas, Universidade Federal do Rio de Janeiro, CCS, Cidade Universitária, Rio de Janeiro, RJ, Brazil.

* To whom correspondence should be addressed: ejbarreiro@ccsdecania.ufrj.br

Table of Contents

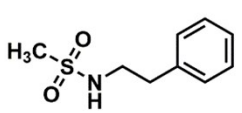

Mpro-x0072

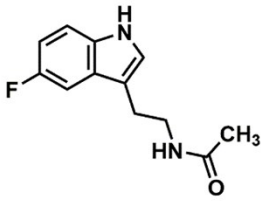

Mpro-x0104

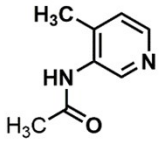

Mpro-x0107

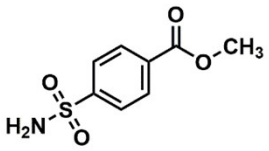

Mpro-x0161

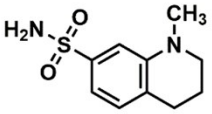

Mpro-x0195

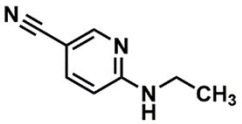

Mpro-x0305

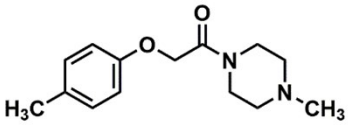

Mpro-x0354

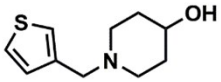

Mpro-x0387

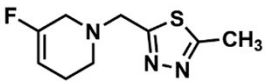

Mpro-x0395

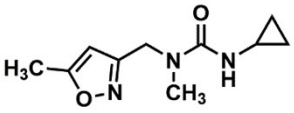

Mpro-x0397

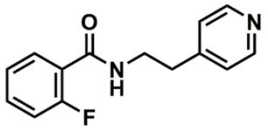

Mpro-x0426

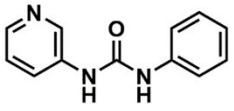

Mpro-x0434

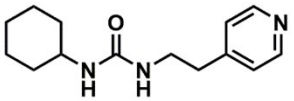

Mpro-x0540

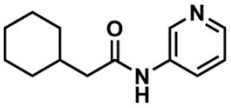

Mpro-x0678

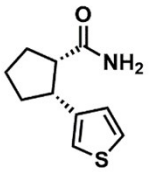

Mpro-x0874

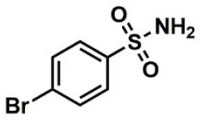

Mpro-x0946

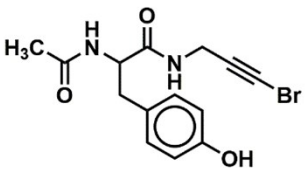

Mpro-x0967

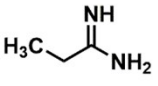

Mpro-x0991

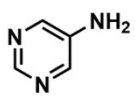

Mpro-x0995

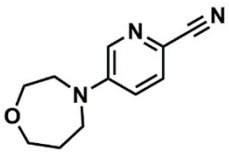

Mpro-x1077

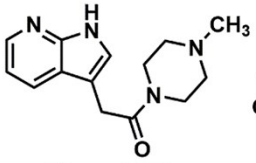

Mpro-x1093

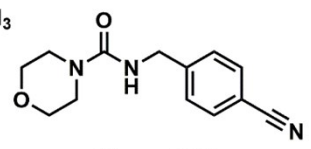

Mpro-x1249

Scheme S1.

Table S1. Interaction overview of the 22 non-covalent fragments co-crystallized with M^{PRO}.

Fragment	Interactions of hydrophobic nature[a]	Strong (S)[b] and weak (w)[c] Hydrogen Bond interactions
x0072	His41 (π)	Ser46 (w)
x0104	His41 (π)	Glu166 (S), Thr190 (w)
x0107	-	Glu166 (S), His163 (S), Phe140 (w)
x0161	-	Glu166 (S), Pro168 (w), Asp187 (w), H_2O154 (S)
x0195	-	H_2O154 (S), Pro168 (w), Met49 (w), H_2O190 (w)
x0305	His41 (π)	Gln189 (S), Met165 (w), H_2O190 (w)
x0354	-	H_2O295 (S), Met165 (w), H_2O217 (w)
x0387	His41 (π)	H_2O343 (S,w), Cys44 (S), H_2O188 (s)
x0395	-	-
x0397	-	H_2O342 (S,w), His163 (S), Cys145 (S), Gly143 (S), His164 (w)
x0426	-	Phe140 (w,w), His163 (S), Cys145 (w), Glu166 (w)
x0434	His41 (π)	H_2O342 (S,S), His163 (S), Glu166 (S), Phe140 (w)
x0540	-	Phe140 (w), His163 (S), Cys145 (w), H_2O316 (S)
x0678	-	His163 (S), Glu166 (S), Phe140 (w), H_2O154 (S)
x0874	His41 (π)	Glu166 (S), Glu166 (S), H_2O270 (S)
x0946	-	Glu166 (S), Pro168 (w), H_2O154 (S)
x0967	-	Phe140 (S), His163 (S), Glu166 (S), Cys145 (w), H_2O342 (S)
x0991	-	Cys44 (S,S), His41 (S)
x0995	-	Asn142 (w), His163 (S), Glu166 (w), Cys145 (w), H_2O155 (S)
x1077	His41 (π)	Glu166 (S), Thr25 (S), His41 (w)
x1093	-	Glu166 (S), Gly189 (w), H_2O154 (S), Met165 (w,w), His163 (S)
x1249	His41 (π)	H_2O342 (S)

a – π-π stacking interaction; b – strong hydrogen bond is characterized by an interaction of an oxygen or nitrogen atom with a hydrogen atom bound to an oxygen or nitrogen atom; c – weak hydrogen bond is characterized by an interaction of an oxygen or nitrogen atom with a hydrogen atom bound to a carbon atom.

Table S2. Linker size profile and distances between linker's central atom and atom/subunit that Interacts with His41 and/or His163 of the 22 non-covalent fragments co-crystallized with M^{PRO}.

Fragment	Size of the linker[a]	Distances between central atom of the linker and aromatic subunit interacting with His41[b]	Distances between central atom of the linker and atom interacting with His163
x0072	0	I	D
x0104	0	I	D
x0107	0	D	I
x0161	0	D	D
x0195	0	D	D
x0305	0	I	D
x0354	3 (2.44 Å)	D	D
x0387	1	3.28 Å	D
x0395	1	D	D
x0397	4 (3.90 Å)	D	3.7 Å / 4.74 Å[e]
x0426	4 (3.28 Å)	D	5.20 Å / 6.51 Å[e]
x0434	3 (2.48 Å)	3.85 Å	4.36 Å
x0540	5 (4.46 Å)	D	5.56 Å
x0678	3 (2.50 Å)	D[f]	4.32 Å
x0874	0	I	D
x0946	0	D	D
x0967	0	D	I
x0991	0	I	D
x0995	0	D	I
x1077	0	I	D
x1093	2 (1.52 Å)	D	3.69 Å (C) / 4.46 Å[e]
x1249	3 (2.50 Å)	4.21 Å	D

a – Only atoms linking two rings (aromatic or not) were considered linkers, the distance between the atoms bonded to each ring is displayed inside parentheses; b – the distance calculated was between the linker atom and the centre of aromatic ring; c – I = interacts with the residue but there is no linker; d – D = do not interacts with the residue; e – Because the linker presented an even number of atoms, the distance was measured for both central atoms; f – x0678 presents a cyclohexane ring bonded to the linker, hence it cannot make aromatic interactions with His41. However, it is oriented to the pocket where other aromatic subunits interacted with His41.

Table S3: Redocking results of the M^{PRO} co-crystalized fragments. The scoring functions with best ranked binding pose RMSD value ≤ 1.6 were considered validated. The RMSD cut-off is the mean value of the crystal structures' resolution.

Fragment	ChemPLP	Goldscore	Chemscore	ASP
x0072	6.6	5.3* (0.5)	5.7	4.9
x0104	6.5	6.8	6.9	6.8
x0107	**0.5**	**0.7**	4.9	4.5
x0161	5.8	2.8	7.4	7.0
x0195	**0.9**	**1.4**	**0.7**	7.2
x0305	7.4	**1.5**	7.3	7.5
x0354	7.6	7.8	7.3	7.4
x0387	2.2	2.6	2.5	**0.8**
x0395	2.1	2.8	3.8	5.4
x0397	4.0	**0.5**	**0.6**	**1.1**
x0426	5.4* (0.7)	5.6* (0.9)	6.0* (0.7)	6.6
x0434	**0.5**	**1.0**	**0.5**	**0.6**
x0540	4.7* (0.5)	6.8	7.2* (0.7)	6.8* (0.5)
x0678	6.1	**0.6**	1.4	3.0
x0874	**0.5**	5.2	**0.8**	**0.6**
x0946	**1.2**	1.7	**1.4**	5.1
x0967	3.5	3.8	4.4	5.0
x0991	**1.3**	2.5	3.9	**1.0**
x0995	**0.6**	**1.5**	**1.1**	**0.7**
x1077	**1.6**	6.4	1.7	2.6
x1097	**0.5**	**0.4**	9.6	8.8
x1249	8.0	4.2	7.4	7.4

* Redocking poses considered validated because the rings fitted the pockets next pharmacophore residues (Fig. S1), presenting RMSD between rings < 1 (indicated on the table), even though the flexible parts were not superimposed.

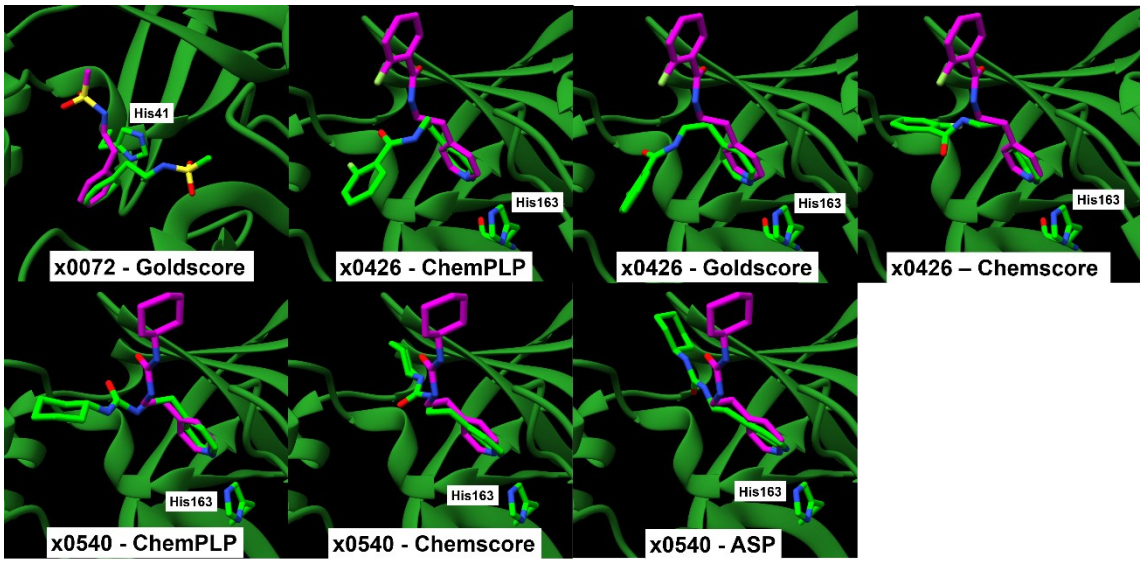

Figure S1. Redocking poses of fragments interacting with residues of the pharmacophore model. x0072 fitted the sub-pocket S2 next to His41, and x0426 and x540 fitted sub-pocket S1 next to His163.

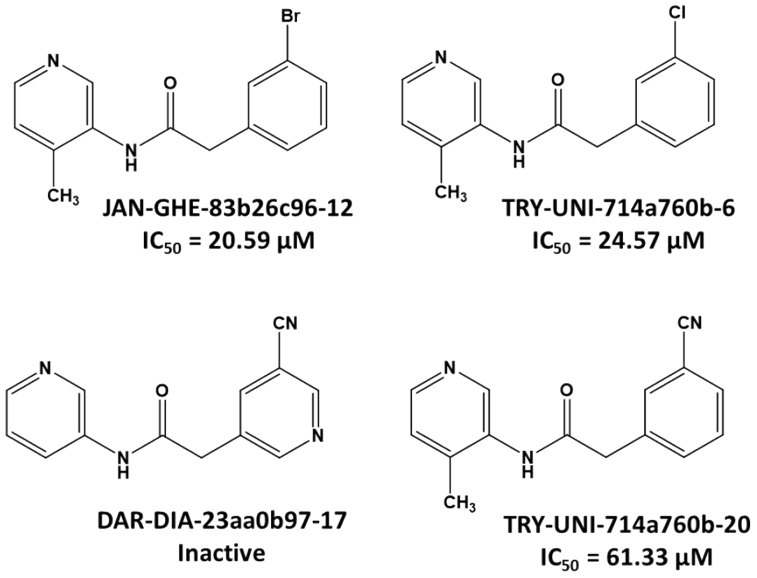

Figure S2. M^{PRO} activity of these four derivatives indicates that the increase in hydrophobicity of the aromatic ring that interacts with His041 correlates with an increase in inhibitory activity.

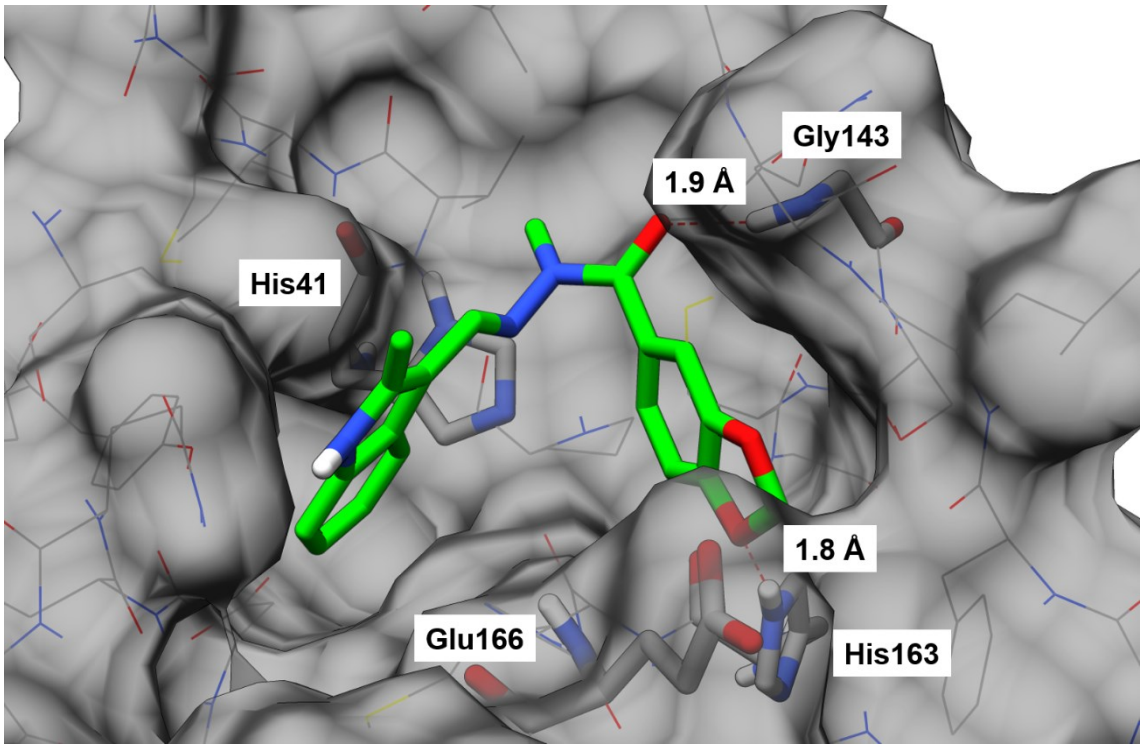

Figure S3. Docking pose of LASSBio-1649 (**13**).

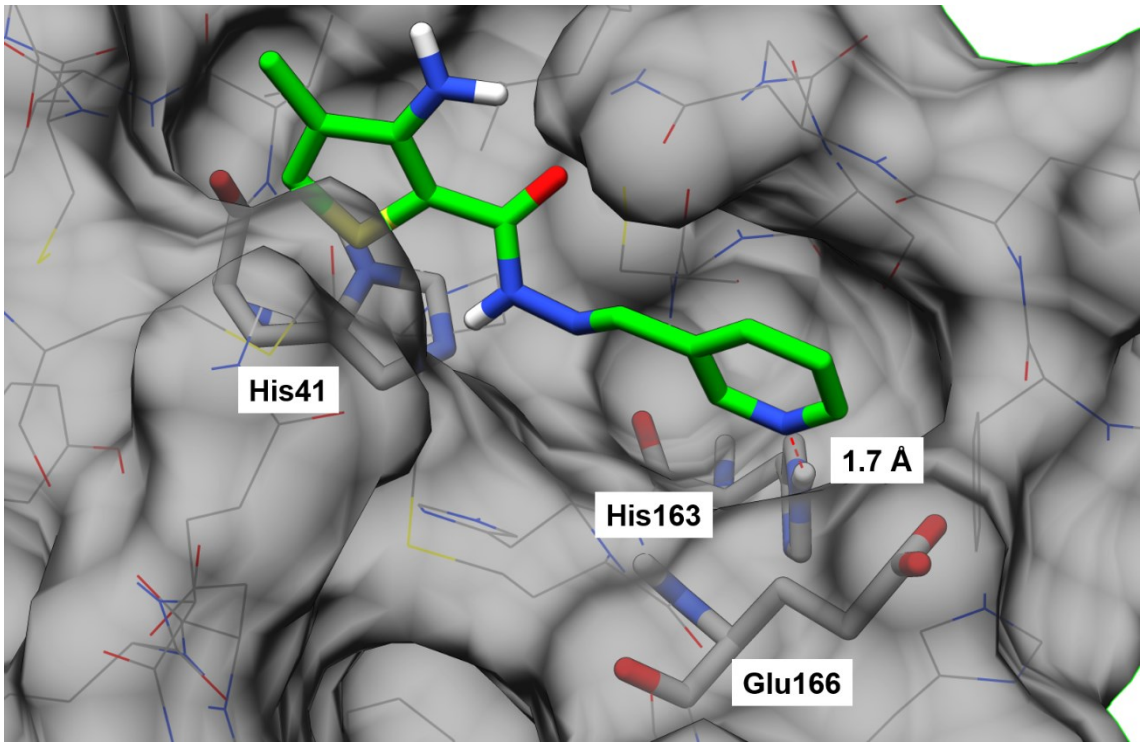

Figure S4. Docking pose of LASSBio-1891 (**14**).

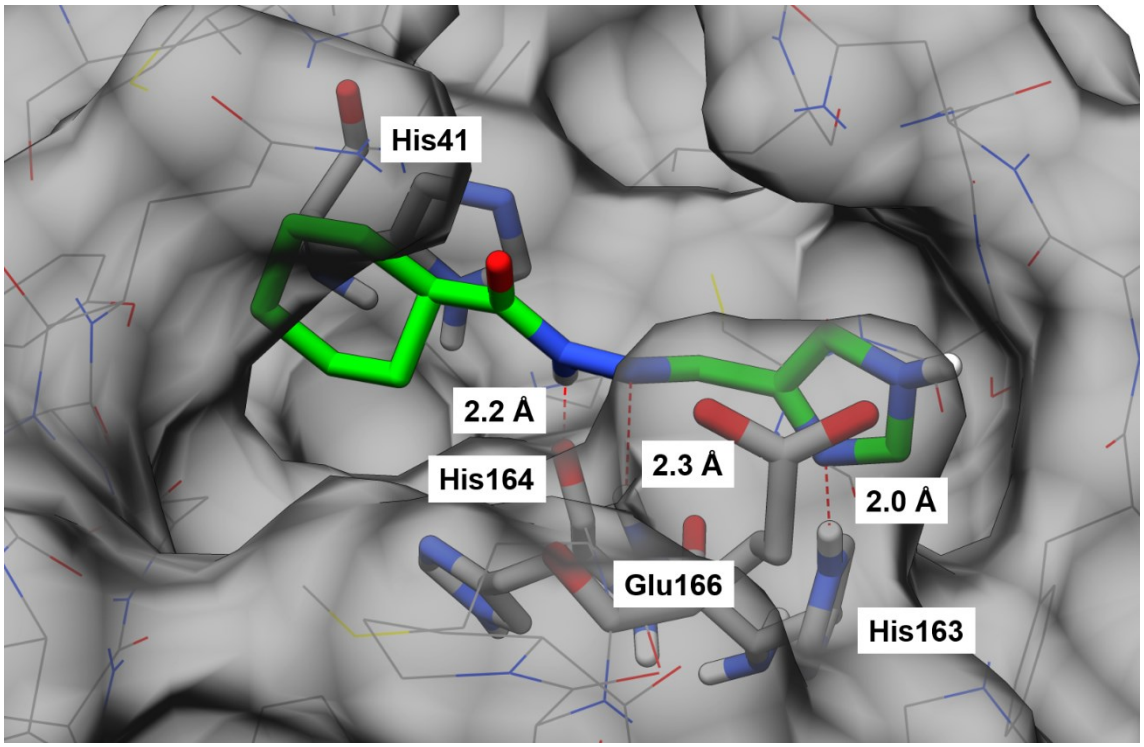

Figure S5. Docking pose of LASSBio-1600 (**15**).

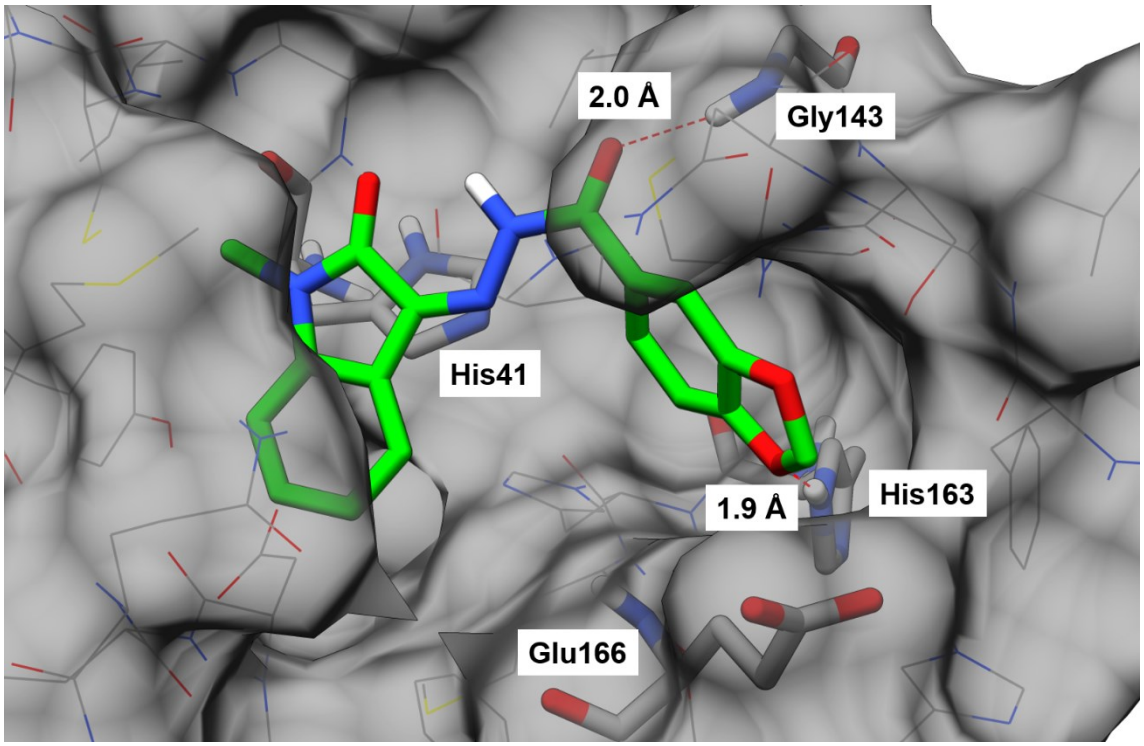

Figure S6. Docking pose of LASSBio-1652 (**16**).

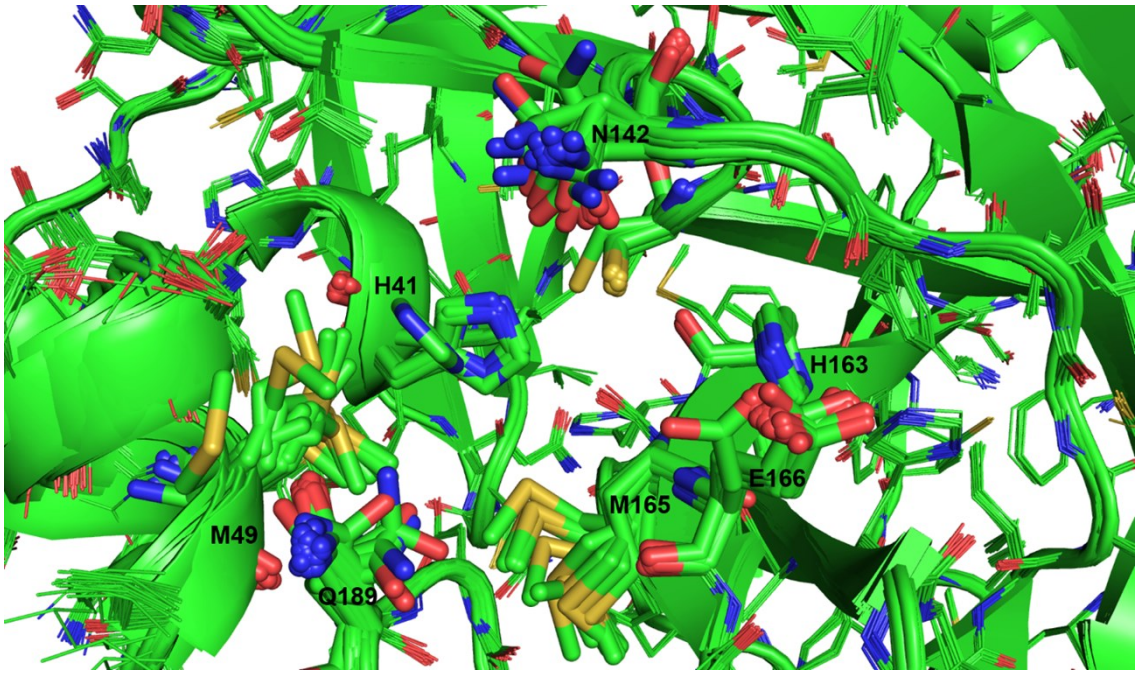

Figure S7. Superimposition of the active site of M^{PRO} obtained from co-crystal structures with non-covalent fragments. Visual inspection of the superimposed structures allowed the identification of amino acid residues which its side chains adopt different conformations to allow the molecular recognition of the co-crystalized fragments shown in Scheme 1 (flexible amino acids highlighted as sticks and remaining residues shown as lines). Based on this analysis, the side chains of binding site residues His41, Met49, Asn142, Cys145, Met165, Glu166 and Gln189 were set with free flexibility.

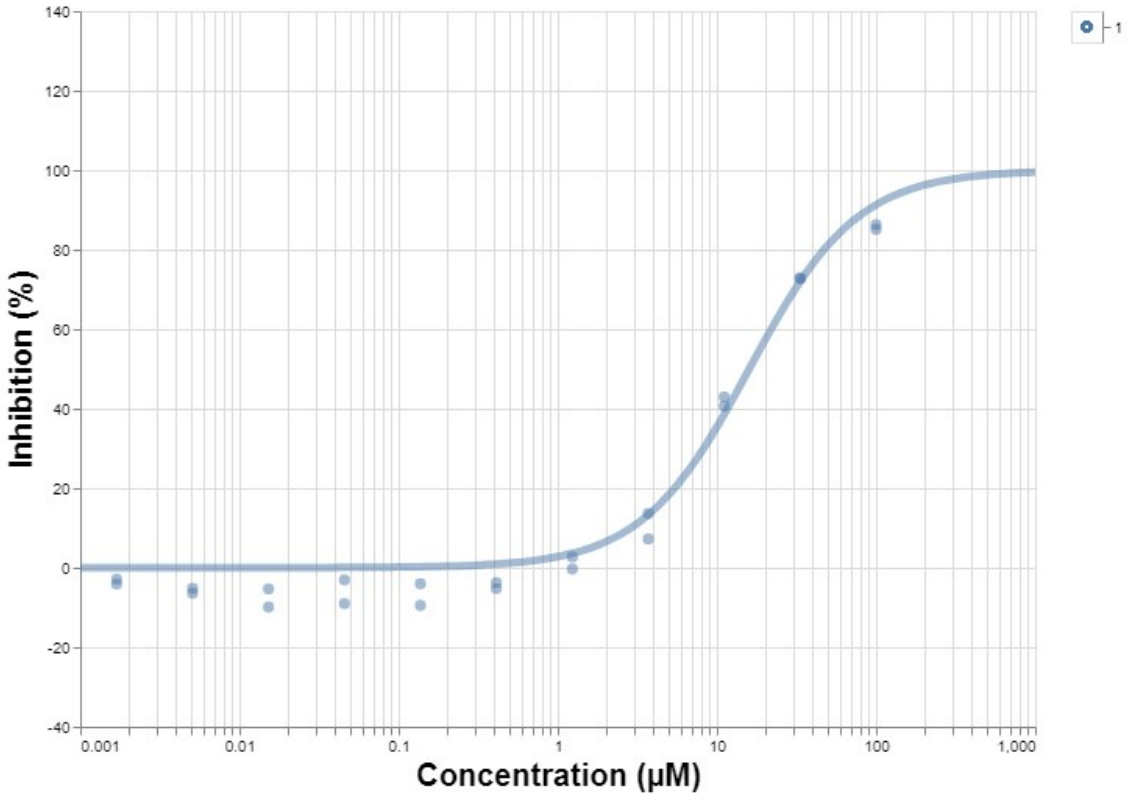

Figure S8. Dose-response curve of LASSBio-1945 (**9**).